Neural Computing and Applications
https://doi.org/10.1007/s00521-021-05925-8

ORIGINAL ARTICLE

Assessment of cement characteristics affecting rheological properties of cement pastes

Ali Mardani-Aghabaglou[1] · Murat Kankal[1] · Sinan Nacar[2] · Burak Felekoğlu[3] · Kambiz Ramyar[4]

Received: 19 March 2020 / Accepted: 11 March 2021
© The Author(s), under exclusive licence to Springer-Verlag London Ltd., part of Springer Nature 2021

Abstract

In this study, the cement-based parameters affecting CEMI portland cements-polycarboxylate ether-based high-range water-reducing (HRWR) admixtures compatibility were investigated. For this purpose, eight CEMI cements and three commercial HRWR admixtures were used. The rheological properties of 112 paste mixtures with different admixture dosages and water/cement (W/C) ratios were determined in accordance with Herschel–Bulkley model. Then after, using the experimental data, proper models were established to predict the dynamic yield stress and final viscosity of the pastes. In addition to cement characteristics (such as fineness, compound composition and equivalent alkali content), water-reducing admixture content and its solid material content as well as water/cement ratio of the pastes were considered as input data. Multivariate adaptive regression splines (MARS) and multiple additive regression trees (MART) methods were used in the models. Besides, artificial neural network (ANN) and conventional regression analysis (CRA) including linear, power, and exponential functions were applied to determine the accuracy of the heuristic regression methods. Three statistical indices, root-mean-square error, mean absolute error, and Nash–Sutcliffe, were used to evaluate the performance of the models. Modeling findings indicated that the model with the lowest error for both of the rheological variables in the testing set is the MART, followed by ANN, MARS, and CRA-Exponential methods. The most effective cement characteristics causing incompatibility, hence detraction of paste rheological properties, in decreasing order, were determined as cement fineness, C_3S, C_3A and equivalent alkali contents. C_4AF and C_2S contents of the cement were found to have less effect on the cement–admixture incompatibility. It will be possible to determine the rheological properties of mixtures containing different cements without conducting an experimental study by using the model based on MART method.

Keywords Cementitious systems · Rheological properties · Multivariate adaptive regression splines · Multiple additive regression trees

1 Introduction

Among the admixtures used in concrete, water-reducing admixtures are the most used ones. The chemical admixtures used in concrete (at least in theory) might have no adverse effect along with the desirable effects on concrete properties [1–6]. The negative effects observed in the mixtures of proper concrete and chemical admixture are attributed to the cement–admixture incompatibility [7]. The most common features of such incompatibility are detraction of rheological properties, acceleration or retarding of setting, segregation, rapid slump loss and increase in shrinkage of the concrete [8–12]. The adverse effects resulting from cement–superplasticizer interaction were found to be arisen in part from cement or plasticizer

✉ Murat Kankal
mkankal@uludag.edu.tr

1 Department of Civil Engineering, Bursa Uludağ University, Nilüfer-Bursa, Turkey

2 Department of Civil Engineering, Tokat Gaziosmanpaşa University, Tokat, Turkey

3 Department of Civil Engineering, Dokuz Eylul University, Buca-Izmir, Turkey

4 Department of Civil Engineering, Ege University, Bornova-Izmir, Turkey

Published online: 02 April 2021

admixture and in part from mix proportions, temperature and ambient conditions [12, 13]. The incompatibility resulting from cement properties was reported to be due to the chemical composition of cement, morphology and structure of C_3A, C_3A/C_4AF ratio, cement fineness, its alkali content and the type and amount of calcium sulfate interground with the clinker [14]. Within this context, the chemical composition of admixture, its main chain length, side chain number and length, anionic/nonionic mole ratio, molecular weight, intermolecular bond structure, density, adsorption property, time of its addition into the concrete mixture, and the amount of admixture added to the concrete are of vital importance [9, 12, 13, 15–20]. The compatibility between admixture and cement reduces the admixture requirement for a given workability and enables production of concrete mixtures having desired properties at a low cost.

Low C_3A cements are known to be desirable in terms of paste rheology [21]. Prince et al. [22] stated that the ettringite resulting from C_3A-sulfate ion hydration consumes most of the water of the cementitious mixture resulting in a considerable reduction in its workability.C_3A compound of the cement can be in either cubic or orthorhombic form [13]. Cubic C_3A is more reactive than the orthorhombic one [21]. Therefore, the presence of majority of C_3A in cubic form results in the rapid formation of ettringite in the cementitious system and makes the control of its rheological properties easy [23]. Moreover, it is stated that the fresh state and rheological properties of the cementitious mixtures improve with the reduction of cement alkali content [8].

Since increasing the fineness of cement increases the surface/volume ratio of the particles, the finer is the cement the higher is the paste viscosity. Thus, for a given consistency, the demand for water-reducing admixture increases [9, 13]. Besides, according to Ramachandran [13], viscosity of the cementitious mixture depends also on the type of calcium sulfate interground with clinker during manufacturing of the cement.

Although there are different opinions about the mechanism of interaction between cement and admixture, it is commonly believed that the chemical composition, structure, and molecular weight of the admixture, as well as the time and method of its addition to the cementitious system, affect strongly the cement–admixture interaction [24–29].

Intensive studies have been carried out, especially at laboratory scale, to investigate the complex behavior of the cementitious systems. In order to facilitate this process, which is quite troublesome in terms of money and time, many modeling studies were also conducted using the available experimental data. In these modeling studies, mostly mechanical properties of cementitious systems such as compressive strength [30–45], ultimate bond strength [46], elastic modulus, split tensile strength, and flexural strength [47–50] or other properties such as slump [33, 36], ultrasonic pulse velocity [51], V-funnel time, slump flow and L-box ratio [35, 52], slump and density of lightweight concrete [53], the expansion of the concrete caused by alkali aggregate reactivity [54], penetrability properties of cement-stabilized clay exposed to sulfate attack [55], and creep strain of ground granulated blast furnace slag concrete [56] were intended to be estimated. Shahriar and Nehdi [57] established models of rheological properties of oil well cement slurries. As it can be observed, the number of studies predicting the rheological properties of cementitious systems is very limited.

Regression analysis is a statistical approach that tries to reveal the relationship between two or more variables with a cause–effect relationship. Regardless of linearity of the model, the mentioned approach is based on the assumption that the dependent variable is normally distributed. MARS and MART heuristic regression techniques used in this study are nonparametric regression methods that make no assumptions about the underlying functional relationship between dependent and independent variables. MARS which is an innovative and promising modeling tool is used as a flexible and fast method for making predictions [58]. The main advantages of MARS are its capacity to capture the intrinsic complicated relationship in high-dimensional data patterns, produce simple and easier-to-interpret models, and predict the contributions of the input variables [59, 60]. Friedman and Meulman [61] proposed a data-driven approach known as MART. This approach was built on a strong powerful framework called Gradient Boosting. Fu et al. [62] emphasized that the MART model is fast, resistant to overfitting, can automatically select valuables, and is a good at handling data imperfection (outliers, missing values, and mistypes).

The methods most commonly selected for modeling of the cementitious systems are regression and artificial intelligence [30–57]. These methods used in the modeling studies are given in detail in Table 1. During the past decade, heuristic regression models such as M5 Tree, support vector regression (SVR), and multivariate adaptive regression splines (MARS) were used for estimation of the cementitious systems properties. Cheng and Cao [49] modeled the strength of the rubberized concrete through MARS, MARS–artificial bee colony, artificial neural network (ANN) and Genetic Programming methods. Chou et al. [38] modeled the strength of concrete using ANN, support vector machine and regression in addition to multiple additive regression trees (MART) and bagging regression trees methods. Dutta et al. [40] compared the MARS model with learning machine and adaptive neuro-fuzzy inference systems models for the estimation of self-compacting concrete (SCC) compressive strength. Kaveh

Table 1 The models used in previous studies

Author(s)	Models*													
	CRA	ANN	Hybrid ANN	MARS	M5Tree	SVR	FL	SVM	Hybrid SVM	MART	ANFIS	ELM	Hybrid MARS	Other
Özcan et al. [30]		*					*							
Saridemir et al. [31]		*					*							
Zhang et al. [32]														*
Amlashi et al. [33]		*		*	*									
Asteris and Mokos [34]		*												
Saha et al. [35]						*								
Selvaraj and Sivaraman [36]									*					
Ashrafian et al. [37]	*	*		*		*							*	
Chou et al. [38]	*	*						*		*				*
Yuan et al. [39]			*								*			
Dutta et al. [40]				*							*	*		
Eskandari-Naddaf and Kazemi [41]														
Yaseen et al. [42]				*	*	*								
Al-Shamiri et al. [43]		*										*		
Ghanizadeh et al. [44]		*						*						
Nguyen et al. [45]		*	*											
Hoang et al. [46]						*								*
Xu et al. [47]	*	*												
Gholampour et al. [48]				*	*	*								
Cheng and Cao et al. [49]			*	*									*	*
Karthiyaini et al. [50]	*	*												
Ashrafian et al. [51]	*	*		*	*	*								
Kaveh et al. [52]				*	*									
Rezaie and Sadighi [53]	*										*			
Yu et al. [54]									*					
Sezer et al. [55]	*	*									*			
Sadowski et al. [56]			*											
Shahriar and Nehdi [57]	*	*												

**CRA* classic regression analysis, *ANN* artificial neural network, *MARS* multi-adaptive regression splines, *SVR* support vector regression, *FL* fuzzy logic, *SVM* support vector machine, *MART* multi-additive regression trees, *ANFIS* adaptive neuro-fuzzy inference systems, *ELM* extreme learning machine

et al. [52] modeled the compressive strength, V-funnel time, slump flow, and L-box ratio of SCC containing fly ash using M5 Tree and MARS methods. Yaseen et al. [42], Gholampour et al. [48], and Ashrafian et al. [51] used MARS, M5 Tree, and SVR models in their studies to estimate the compressive strength of various special concrete mixtures. Amlashi et al. [33] established MARS and M5 Tree models for modeling the slump, compressive strength, and elastic modulus of bentonite plastic concrete and compared the results with those of the ANN model. Zhang et al. [32] modeled the compressive strength of lightweight SSC with hybrid beetle antennae search algorithm-based random forest method. The literature survey revealed that, except for one study where MART was

applied, in recent years MARS method was most commonly preferred for modeling of the cementitious system properties (Table 1).

The main objective of this study is to determine the parameters affecting cement–admixture compatibility in order of influence rate. Another aim of the study is to predict the rheological properties of other different cementitious systems without any experimental study by using the presented model based on the data obtained from the experiments within the scope of the study. For this purpose, rheological characteristics (dynamic yield stress, DYS and final viscosity, FV) of the paste mixtures containing high-range water-reducing (HRWR) admixture were taken into consideration and modeled with MARS and MART heuristic regression methods. The performance of the models was determined regarding the conventional regression analysis (CRA) and ANN results.

Using eight ordinary (CEM I) portland cements and three polycarboxylate ether-based HRWR admixtures in three different ratios, 112 paste mixtures having two different W/C ratios were prepared. The effects of cement fineness, proportions of cement major compounds, and equivalent alkali content of the cement (EAC) as well as water-reducing admixture content (AC), admixture solid content (ASC), and water/cement ratio of the mixture (W/C) on the rheological properties of pastes were investigated.

In Sect. 2, the experimental study is presented. The methodology of modeling is described in Sect. 3. The results and discussion are given in Sect. 4. Lastly, conclusion part appears in Sect. 5.

2 Experimental study

2.1 Materials and mix proportions

Eight ordinary portland cements, conforming to EN 197-1 Standard, provided from 5 Turkish cement plants were used. In the production of cements, five calcium sulfate dihydrate brands having SO_3 contents in the range of 38 to 40% were used as retarder. The properties of cements are given in Table 2. Three polycarboxylate ether-based HRWR admixtures conforming to EN 934-2+A1 Standard were used. Properties of the admixtures provided from their producers are presented in Table 3.

Six series of paste mixtures, having 0.32 and 0.35 W/C ratios and containing 0%, 0.1%, and 0.2% admixture (by weight of cement), for each cement–admixture couple were prepared. In this way, the rheological properties of 112 paste mixtures were examined. The admixture requirement was found to be negligible in the mixtures having W/C ratio beyond 0.35. Meanwhile, the mixtures with W/C ratio lower than 0.32 were too stiff to be mixed homogeneously even by the admixture addition. Thus, pastes of 0.32 and 0.35 W/C ratios were studied in the present study. Indeed, 0.33 W/C ratio was also tested. However, the mixtures with 0.32 and 0.33 W/C ratios exhibited considerably close rheological behavior; hence, the rheological parameters of the 0.33 W/C ratio mixtures were not considered in this paper. The mixtures were designated in terms of their W/C ratio, cement, and admixture type. For instance, the mixture containing C1 cement with 0.32 W/C ratio and SP-1 admixture is designated as C1-0.32-SP1.

2.2 Test method

A rheometer supported by Ball Measuring System (BMS) and equipped with Rheoplus software (and some additional microprograms) was used for the measurements of static and dynamic rheological properties [2, 3, 63–66]. The details of measurement of rheological properties can be found elsewhere [64, 66]. A deformation rate history consisting of four periods, as shown in Fig. 1, was found to be suitable for determination of the rheological properties of the mixtures. Factors such as capacity of the rheometer, maximum admixture usability, and a full turn of the rheometer ball were taken into account in the selection of the deformation rate history. In the first stage, the flow curves were obtained by applying various shear rates to the pastes. The intersections of the flow curves, obtained in the fourth period (Fig. 1), with stress axis were accepted as the dynamic yield stress of the mixtures. In the second stage, static yield stress of the mixtures was determined with no pretreatment at considerably low deformation rates. At this stage, the resistances of mixtures to the ball movement in the first stage were measured. Using these shear stress values, yield stress–time diagrams were plotted for each paste. The maximum yield stress in this diagram was chosen as the static yield stress of the mixture.

As it was stated earlier [64], at low shear rates the viscosity value measured in Herschel–Bulkley model mostly decreases with increasing shear rate. However, beyond a definite shear rate, it remains nearly constant, called "final viscosity." Owing to the fact that most of the mixtures of the present study showed a stable flow curve at shear rates beyond 30 s^{-1}, the instant apparent viscosity of the mixtures at 30 s^{-1} shear rate was accepted as their final viscosity.

Table 2 Chemical composition and physical properties of cements

	C-1	C-2	C-3	C-4	C-5	C-6	C-7	C-8
SiO_2	19.85	18.77	18.95	19.03	21.88	19.01	18.21	18.65
Al_2O_3	4.41	3.67	3.66	4.08	3.76	2.82	3.97	5.09
Fe_2O_3	4.14	5.05	4.95	3.42	4.05	4.64	3.17	2.45
CaO	61.05	64.27	63.91	64.84	62.58	64.28	64.39	63.75
MgO	1.68	1.38	1.52	1.48	1.56	1.42	1.17	2.35
Na_2O	0.27	0.20	0.24	0.28	0.63	0.72	0.42	0.64
K_2O	0.50	0.62	0.41	0.63	0.63	0.74	0.70	0.90
SO_3	3.16	3.17	2.81	3.10	2.47	3.00	2.95	2.72
Cl^-	-	0.006	0.006	0.005	0.007	0.007	0.005	-
Free CaO	1.37	1.42	1.97	1.93	1.22	0.91	1.41	1.51
LOI	3.30	1.40	1.64	1.37	0.70	2.53	3.3	1.77
Total	99.73	99.96	100.06	100.16	99.49	100.08	98.99	99.83
Specific gravity	3.14	3.16	3.16	3.14	3.15	3.2	3.11	3.11
Blaine specific surface (cm^2/g)	4260	3820	3760	3900	2810	3810	3090	3510
Residual on 0.090 mm sieve (%)	0.2	0	0	0.2	4.9	0.2	1.3	0.4
Residual on 0.045 mm sieve (%)	1.4	1.7	2	11.4	21.5	0.3	-	-
Residual on 0.032 mm sieve (%)	6.6	7.2	7.9	20.7	33.6	7.3	21.4	2.7
Setting time (hour)								
Initial	02:50	02:50	03:30	02:25	02:25	02:55	02:50	02:30
Final	05:10	05:15	05:25	03:45	03:35	04:05	04:50	04:05
Normal consistency (%)	30.2	30.8	30.4	28.2	24.6	28.8	27.6	27.2
Chemical composition of clinkers								
Items	K-1	K-2	K-3	K-4	K-5	K-6	K-7	K-8
C_3S	62.83	64.03	65.73	66.15	67.10	61.99	64.21	52.50
C_2S	13.20	12.63	11.05	11.86	10.20	13.31	11.39	20.37
C_3A	5.85	2.77	1.90	6.92	3.58	3.15	7.92	13.88
C_4AF	13.63	15.98	16.27	9.68	13.13	15.23	10.27	7.67

Table 3 Some properties of polycarboxylate ether-based high-range water-reducing admixture

Type	Alkali content (%) (Na_2O)	Density (g/cm^3)	Solids content (%)	Chloride content (%)	pH at 25 °C	Operating* range (%)
SP-1	<5	1.098	33.5	0.012	6.54	0.6–2.0
SP-2	<5	1.099	33.76	0.011	6.60	0.6–2.0
SP-3	0.31	1.075	38.56	0.009	5.68	0.6–2.0

* By weight of cement

3 Methodology of modeling

3.1 Development of models

In addition to the 16 control pastes (prepared from eight cements with two W/C ratios) containing no admixture, 96 test mixtures having two different AC, three different ASC, two different W/C, and containing eight different cements were tested. The results of tests conducted on 112 pastes were used in developing models (Table 4). The results of 80 (about 70%) experiments were used for training, and the remaining 32 (about 30%) were reserved for testing of the models. While creating the testing set, it was paid attention that it represents the whole data group (Table 5). At this point, for example, 32 test data were created by considering four data from each of eight different cement types. In addition, since two different W/C ratios were used in the models, a test set was created with 32 data in total, 16 for

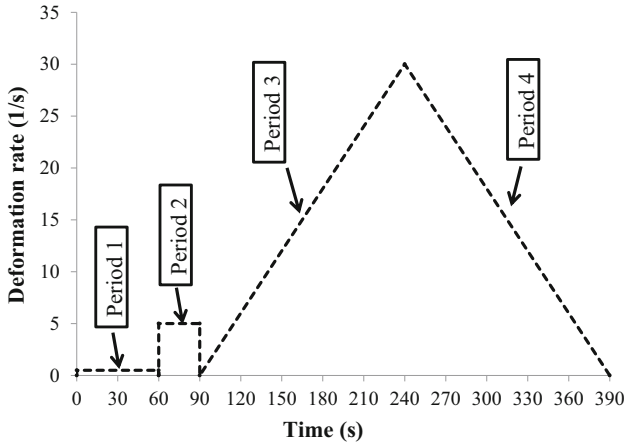


Fig. 1 Deformation history of the paste mixtures

both W/C ratios. A similar selection was made for other input variables.

The CRA method was initially utilized to determine the coefficients of the equations providing the most compatible results with the experimental values of DYS and FV. Three regression functions, i.e., linear (LF), power (PF), and exponential (EF), as shown below, were used to estimate the DYS and FV.

$$y_{\text{Linear}} = w_0 + w_1x_1 + w_2x_2 + w_3x_3 + \cdots + w_nx_n \quad (1)$$

$$y_{\text{Power}} = w_0x_1^{w_1}x_2^{w_2}x_3^{w_3}x_4^{w_4}\cdots x_n^{b_n} \quad (2)$$

$$y_{\text{Exponential}} = w_0 + \exp(w_1 + w_2x_1 + w_3x_2 + \cdots + w_{n+1}x_n) \quad (3)$$

Then, the MARS and MART models were applied to the training data set and the equations and basic functions giving the lowest error were determined. The Salford Predictive Modeler 8.0 software was used for MARS and MART models. Finally, the weights found in the ANN model were determined using training data set.

In order to overcome the difficulty of the optimization of extreme values found in the data set, to facilitate optimization, and to achieve more accurate results, the data were normalized between 0.1 and 0.9 using the following expression [67]:

$$\text{Normalised value} = \left[\frac{\text{Raw value} - \text{Minimum value}}{\text{Maximum value} - \text{Minimum value}}\right] \times (0.8) + 0.1 \quad (4)$$

3.2 Artificial neural networks (ANN)

ANNs are human attempts to simulate and understand what goes on in nervous system, with the hope of capturing some of the power of these biological systems. ANNs are inspired by biological systems with large number of neurons which collectively perform tasks that even the largest computers have not been able to match [68, 69]. Backpropagation algorithm was chosen as the training algorithm in the ANN model. Backpropagation is the most widely used learning algorithm in ANN, as well as one of the most powerful algorithms [70]. The ANN and backpropagation details can be found in the study published by Uzlu et al. [71].

3.3 Multivariate adaptive regression splines (MARS)

MARS is a nonparametric regression method developed by Friedman [58]. The method assumes no functional relationship between dependent and independent variables [59]. In place of this, it applies a divide-and-conquer strategy to explain the relationship among the variables [72]. More details about the MARS and its implementation can be found elsewhere [73–75].

3.4 Multiple additive regression trees (MART)

Being a revolutionary advance in machine learning technology, the stochastic gradient boosting (commonly referred to as gradient boosting) was developed by Friedman [76]. MART is a general additive boosting regression

Table 4 Values of variables used in models

Cement type	CF (cm^2/g)	C_3A (%)	C_3S (%)	C_2S (%)	C_4AF (%)	EAC (%)	AC (%)	ASC (%)	W/C
C1	4260	5.85	62.83	13.20	13.63	0.59900	0	0	0.32
C2	3820	2.77	64.03	12.63	15.98	0.60796	0.1	33.5	0.35
C3	3760	1.90	65.73	11.05	16.27	0.50978	0.2	33.76	
C4	3900	6.92	66.15	11.86	9.68	0.69454		38.56	
C5	2810	3.58	67.10	10.20	13.13	1.04454			
C6	3810	3.15	61.99	13.31	15.23	1.20692			
C7	3090	7.92	64.21	11.39	10.27	0.88060			
C8	3510	13.88	52.50	20.37	7.67	1.23220			

Table 5 Input values of test sets in the model

Cement type	CF (cm^2/g)	C_3A (%)	C_3S (%)	C_2S (%)	C_4AF (%)	EAC (%)	AC (%)	ASC (%)	W/C
C1	4260	5.85	62.83	13.20	13.63	0.59900	0.1	33.50	0.32
							0.2	33.76	0.35
							0.1	38.56	0.32
							0.2	38.56	0.35
C2	3820	2.77	64.03	12.63	15.98	0.60796	0	0	0.35
							0.2	33.50	0.35
							0.1	33.76	0.32
							0.1	38.56	0.32
C3	3760	1.90	65.73	11.05	16.27	0.50978	0.1	33.50	0.35
							0.2	33.76	0.32
							0.1	33.76	0.35
							0.2	38.56	0.32
C4	3900	6.92	66.15	11.86	9.68	0.69454	0	0	0.32
							0.2	33.50	0.32
							0.2	33.76	0.35
							0.1	38.56	0.35
C5	2810	3.58	67.10	10.20	13.13	1.04454	0.1	33.50	0.35
							0.2	33.50	0.35
							0.1	33.76	0.32
							0.2	38.56	0.32
C6	3810	3.15	61.99	13.31	15.23	1.20692	0	0	0.32
							0.1	33.50	0.32
							0.2	33.76	0.35
							0.1	38.56	0.35
C7	3090	7.92	64.21	11.39	10.27	0.88060	0.2	33.50	0.35
							0.1	33.76	0.32
							0.2	33.76	0.35
							0.1	38.56	0.32
C8	3510	13.88	52.50	20.37	7.67	1.23220	0	0	0.35
							0.1	33.50	0.32
							0.1	33.76	0.32
							0.2	38.56	0.35

model (ABRM) with a decision tree as its base learner. The main difference of the MART method with other ABRM is that its basic learner (implemented using the classification and regression tree) is not only a decision tree, but also may provide a nonlinear relationship between features and targets [77]. More details about the MART model can be found in Friedman and Muelman [61] and Li and Goel [78].

3.5 Assessment of model performance

The performance of models was assessed quantitatively with root-mean-square error (RMSE), mean absolute error (MAE), and Nash–Sutcliffe (NS) as follows:

$$\mathrm{RMSE} = \left[\frac{1}{n}\sum_{i=1}^{n}(O_i - P_i)^2\right]^{1/2}. \tag{5}$$

$$\mathrm{MAE} = \frac{1}{n}\sum_{i=1}^{n}|(O_i - P_i)|. \tag{6}$$

$$\mathrm{NS} = 1 - \frac{\sum_{i=1}^{n}(O_i - P_i)^2}{\sum_{i=1}^{n}\left(O_i - \overline{O}\right)^2}. \tag{7}$$

where O_i is the experimental yield stress or final viscosity values, $\overline{O}$ is the mean of these values, P_i is the value obtained from the model and n is number of observations. NS ranges from $-\infty$ to 1. Here, NS = 1 proves that the method is physical and perfect method. Moriasi et al. [79] proposed a range that determines the adequacy level of

model performance for NS statistics. If the NS is 0.75–1, 0.65–0.75, 0.50–0.65, and less than 0.50, it means that the model is very good, good, sufficient, and unsatisfactory, respectively.

4 Results and discussion

4.1 Evaluation of experimental results

4.1.1 Determination of rheological properties of cement paste mixtures

As stated earlier, the dynamic yield stress (DYS), static yield stress (SYS), and final viscosity (FV) values were determined in this study as rheological properties of the mixtures.

4.1.2 Dynamic yield stress and final viscosity of the paste mixtures

Rheological properties of the paste mixtures are summarized in Tables 6, 7, 8, 9, 10, 11, 12, and 13. As it can be seen from Table 6, irrespective of w/c ratio, admixture type, and content, it was determined that the dynamic yield stress and final viscosity values were varied between 36 and 111 Pa and 3 and 11 Pa.s, respectively, for C1 mixtures. These ranges were determined as 7–82 Pa, 9–1 Pa.s and 0.1–75 Pa, 5–82 Pa.s for C2 and C3 mixtures, respectively (Tables 7 and 8). As expected, irrespective of cement and admixture type, DYS, SYS, and FV values of the mixtures reduced upon increasing either W/C ratio or admixture content of the mix. It was reported earlier that the fineness of cement, solubility of sulfate found in cement, and (to a lower extent) C_3A and C_4AF contents are the most effective parameters on the rheological properties of the high-performance concretes with low W/C ratios [1]. The pastes investigated in the present study have also low W/C ratios (0.32 and 0.35). Compared to those of the control mixtures containing no admixture, yield stress and FV values in (almost) all of the admixture-bearing mixtures reduced. However, in spite of the presence of admixture, C4-0.32-SP1 and C4-0.32-SP2 mixtures showed greater DYS and FV values than those of their counterpart control mixtures (Table 9). It should be noted that for the sake of time saving, during the preparation of the mixtures, first the control pastes containing no admixture were prepared and tested. Then, immediately 0.1wt% admixture was added to the paste and thoroughly mixed to obtain homogeneity. After testing the resultant mixtures, further 0.1wt% admixture was added to mix and the same procedure was repeated. Thus, the time of addition of the admixture and increasing its content to 0.2% was around 10 to 20 min after the preparation of the control mixtures. Indeed, the control mixtures were prepared three times before the addition of each admixture. Due to the small variation in ambient conditions, negligible differences were observed between the results of the repeated tests. Since during

Table 6 Rheological properties of C1 pastes

Mix	Rheological properties		Admixture dosage (wt% of cement)		
			0%	0.1%	0.2%
C1-0.32-SP1	Yield stress (Pa)	Dynamic	102.43	88	44.25
		Static	1738	185.4	79.3
	Final viscosity (Pa.s)		11.65	8.39	4.22
C1-0.35-SP1	Yield stress (Pa)	Dynamic	67.45	75.3	36.3
		Static	289	104.1	56.4
	Final viscosity (Pa.s)		6.25	5.8	4.05
C1-0.32-SP2	Yield stress (Pa)	Dynamic	102.43	97.28	96.16
		Static	1295	305.8	142.5
	Final viscosity (Pa.s)		11.65	9	6.07
C1-0.35-SP2	Yield stress (Pa)	Dynamic	67.45	64.53	42.8
		Static	452.5	92.1	56.5
	Final viscosity (Pa.s)		6.25	4.56	2.94
C1-0.32-SP3	Yield stress (Pa)	Dynamic	102.43	111.27	103.26
		Static	686	335	169.5
	Final viscosity (Pa.s)		11.65	9.85	7.07
C1-0.35-SP3	Yield stress (Pa)	Dynamic	67.45	80.41	43.98
		Static	274	98.8	65.1
	Final viscosity (Pa.s)		6.25	4.77	3.15

Table 7 Rheological properties of C2 pastes

Mix	Rheological properties		Admixture dosage (wt% of cement)		
			0%	0.1%	0.2%
C2-0.32-SP1	Yield stress (Pa)	Dynamic	82.44	75.3	36.3
		Static	1278	155.9	58.8
	Final viscosity (Pa.s)		9.68	5.8	4.05
C2-0.35-SP1	Yield stress (Pa)	Dynamic	50.56	36.7	7.71
		Static	155.6	63.9	12.5
	Final viscosity (Pa.s)		5.71	3.6	1.11
C2-0.32-SP2	Yield stress (Pa)	Dynamic	82.44	67.54	33.14
		Static	562	161.6	73.4
	Final viscosity (Pa.s)		9.68	4.42	2.98
C2-0.35-SP2	Yield stress (Pa)	Dynamic	50.56	27.09	17.99
		Static	308	39.8	15.5
	Final viscosity (Pa.s)		5.71	2.28	1.35
C2-0.32-SP3	Yield stress (Pa)	Dynamic	82.44	58.73	36.6
		Static	681	172.4	40.7
	Final viscosity (Pa.s)		9.68	4.1	2.6
C2-0.35-SP3	Yield stress (Pa)	Dynamic	50.56	35.7	20.5
		Static	265.3	61.3	14.9
	Final viscosity (Pa.s)		5.71	2.56	1.98

Table 8 Rheological properties of C3 pastes

Mix	Rheological properties		Admixture dosage (wt% of cement)		
			0%	0.1%	0.2%
C3-0.32-SP1	Yield stress (Pa)	Dynamic	75.64	58.73	8.21
		Static	461.6	63.5	11.96
	Final viscosity (Pa.s)		6.17	4.1	1.95
C3-0.35-SP1	Yield stress (Pa)	Dynamic	46.63	12.62	0.1
		Static	81.7	18.5	1.86
	Final viscosity (Pa.s)		4.16	1.15	0.23
C3-0.32-SP2	Yield stress (Pa)	Dynamic	75.64	47.8	13.97
		Static	438	75	24
	Final viscosity (Pa.s)		6.17	4.25	2.34
C3-0.35-SP2	Yield stress (Pa)	Dynamic	46.63	18.94	4.38
		Static	150	25.5	6.6
	Final viscosity (Pa.s)		4.16	2.22	0.94
C3-0.32-SP3	Yield stress (Pa)	Dynamic	75.64	39.61	3.97
		Static	420.5	68.4	12.84
	Final viscosity (Pa.s)		6.17	4.91	1.96
C3-0.35-SP3	Yield stress (Pa)	Dynamic	46.63	11.48	2.57
		Static	150.8	18.4	2.97
	Final viscosity (Pa.s)		4.16	1.55	0.58

modeling only one value is to be assigned for each variable, average of the control mix properties was reported and taken into consideration in modeling. Table 2 reveals that the C4 cement has a high Blaine fineness (3900 cm^2/g) and a relative high C_3A content (6.92%). Owing to the rapid hydration rate of fine cements, it seems that the rigidity occurred in C4-bearing pastes before the addition of the superplasticizer was so high that SP-1 and SP-2 admixtures were not able to overcome it and improve the rheological properties of the paste. This is in some way an indication of incompatibility between the cement and admixture. This was not the case in SP-3-bearing C4

Table 9 Rheological properties of C4 pastes

Mix	Rheological properties		Admixture dosage (wt% of cement)		
			0%	0.1%	0.2%
C4-0.32-SP1	Yield stress (Pa)	Dynamic	46.62	75.24	57.22
		Static	608.7	90.6	86.7
	Final viscosity (Pa.s)		3.48	4.17	3.3
C4-0.35-SP1	Yield stress (Pa)	Dynamic	30.24	19.02	4.14
		Static	46.1	23.7	7.1
	Final viscosity (Pa.s)		2.4	1.65	0.75
C4-0.32-SP2	Yield stress (Pa)	Dynamic	46.62	83.06	44.62
		Static	710.4	103.8	61.5
	Final viscosity (Pa.s)		3.48	4.82	2.98
C4-0.35-SP2	Yield stress (Pa)	Dynamic	30.24	34.28	17.99
		Static	146.2	40.6	26.1
	Final viscosity (Pa.s)		2.4	2.34	1.37
C4-0.32-SP3	Yield stress (Pa)	Dynamic	46.62	35.78	4.59
		Static	124.4	49.9	12.1
	Final viscosity (Pa.s)		3.48	2.75	1.1
C4-0.35-SP3	Yield stress (Pa)	Dynamic	30.24	13.13	3.69
		Static	49.7	21.5	7.1
	Final viscosity (Pa.s)		2.4	1.34	0.68

Table 10 Rheological properties of C5 pastes

Mix	Rheological properties		Admixture dosage (wt% of cement)		
			0%	0.1%	0.2%
C5-0.32-SP1	Yield stress (Pa)	Dynamic	43.46	14.01	2.56
		Static	166.4	19.6	5.4
	Final viscosity (Pa.s)		3.9	1.31	0.77
C5-0.35-SP1	Yield stress (Pa)	Dynamic	21.44	7.65	1.74
		Static	68.6	13.8	1.79
	Final viscosity (Pa.s)		2.19	0.78	0.45
C5-0.32-SP2	Yield stress (Pa)	Dynamic	43.46	10.53	3.85
		Static	138.9	16.4	4.9
	Final viscosity (Pa.s)		3.9	1.28	0.72
C5-0.35-SP2	Yield stress (Pa)	Dynamic	21.44	4.31	2.92
		Static	56.9	11.1	2
	Final viscosity (Pa.s)		2.19	0.66	0.44
C5-0.32-SP3	Yield stress (Pa)	Dynamic	43.46	6.09	1.61
		Static	77.2	6.1	1.62
	Final viscosity (Pa.s)		3.9	0.74	0.44
C5-0.35-SP3	Yield stress (Pa)	Dynamic	21.44	2.24	0.005
		Static	74.3	2.5	0.54
	Final viscosity (Pa.s)		2.19	0.52	0.24

pastes, which was attributed to the C4 cement–SP-3 admixture compatibility.

Being products of the same plant, C1, C2, and C3 cements were manufactured from the same raw materials and same gypsum (obviously in different proportions). As it can be seen from Table 2, C_3A contents of C1, C2, and C3 cements are 5.85%, 2.77%, and 1.90%, respectively. Neglecting the other factors involved, an improvement in the rheological properties of the pastes was expected upon reduction of cement C_3A content (Tables 6, 7, and 8). Indeed, this was the case. C2 pastes either plain or with admixture showed better rheological properties than those

Table 11 Rheological properties of C6 pastes

Mix	Rheological properties		Admixture dosage (wt% of cement)		
			0%	0.1%	0.2%
C6-0.32-SP1	Yield stress (Pa)	Dynamic	85.91	83.4	20.24
		Static	548.7	127.4	56.6
	Final viscosity (Pa.s)		9.78	6.19	3.03
C6-0.35-SP1	Yield stress (Pa)	Dynamic	87.49	47.56	6.82
		Static	360.9	66	18.6
	Final viscosity (Pa.s)		9.15	3.77	1.43
C6-0.32-SP2	Yield stress (Pa)	Dynamic	85.91	98.44	31.99
		Static	240.5	140.1	54.7
	Final viscosity (Pa.s)		9.78	6.3	3.23
C6-0.35-SP2	Yield stress (Pa)	Dynamic	87.49	28.84	6.88
		Static	555.7	43	19
	Final viscosity (Pa.s)		9.15	2.52	1.06
C6-0.32-SP3	Yield stress (Pa)	Dynamic	85.91	89.72	21.14
		Static	850	134.6	58.1
	Final viscosity (Pa.s)		9.78	6.64	3.08
C6-0.35-SP3	Yield stress (Pa)	Dynamic	87.49	36.99	7.3
		Static	547.4	51.5	13.3
	Final viscosity (Pa.s)		9.15	2.84	1.21

Table 12 Rheological properties of C7 pastes

Mix	Rheological properties		Admixture dosage (wt% of cement)		
			0%	0.1%	0.2%
C7-0.32-SP1	Yield stress (Pa)	Dynamic	84.29	36.76	3.47
		Static	179.4	57.5	7.7
	Final viscosity (Pa.s)		6.85	3.9	1.22
C7-0.35-SP1	Yield stress (Pa)	Dynamic	41.68	8.84	1.54
		Static	68.2	16	1.9
	Final viscosity (Pa.s)		3.35	1.46	0.55
C7-0.32-SP2	Yield stress (Pa)	Dynamic	84.29	58.38	14.66
		Static	299.6	76.1	13.2
	Final viscosity (Pa.s)		6.85	5.01	2.05
C7-0.35-SP2	Yield stress (Pa)	Dynamic	41.68	26.83	6.02
		Static	85.1	38.6	14
	Final viscosity (Pa.s)		3.35	2.35	1.01
C7-0.32-SP3	Yield stress (Pa)	Dynamic	84.29	30.54	6.66
		Static	128.2	54.8	11.6
	Final viscosity (Pa.s)		6.85	3.17	1.36
C7-0.35-SP3	Yield stress (Pa)	Dynamic	41.68	11.63	4.3
		Static	42.8	16.1	3.4
	Final viscosity (Pa.s)		3.35	1.19	0.66

of C1-bearing counterparts. Among these cements, C3 with the lowest C_3A content was the most successful one from paste rheological properties viewpoint.

Irrespective of admixture type, C5 cement was found to show the best performance in terms of paste rheological properties (Table 10). This behavior seems to be arisen from its low C_3A content and low fineness. Aïtcin [21] reported that low C_3A cements improve the fluidity of concrete. The fact was attributed to rapid formation of considerable needle-like ettringite upon C_3A + gypsum hydration which consumes a great amount of mixing water and, hence, reduces workability of the cementitious system.

Table 13 Rheological properties of C8 pastes

Mix	Rheological properties		Admixture dosage (wt% of cement)		
			0%	0.1%	0.2%
C8-0.32-SP1	Yield stress (Pa)	Dynamic	98.14	77.6	29.22
		Static	166.36	106.7	48.1
	Final viscosity (Pa.s)		5.97	4.69	2.5
C8-0.35-SP1	Yield stress (Pa)	Dynamic	59.34	30.58	6.99
		Static	77.8	43.6	13.3
	Final viscosity (Pa.s)		3.71	2.22	0.91
C8-0.32-SP2	Yield stress (Pa)	Dynamic	98.14	74.92	27.61
		Static	185.5	93.3	44.1
	Final viscosity (Pa.s)		5.97	4.56	2.49
C8-0.35-SP2	Yield stress (Pa)	Dynamic	59.34	40.09	16
		Static	87.7	57.8	24.9
	Final viscosity (Pa.s)		3.71	2.83	1.53
C8-0.32-SP3	Yield stress (Pa)	Dynamic	98.14	23.98	1.92
		Static	208.3	33.2	5.3
	Final viscosity (Pa.s)		5.97	2.41	0.86
C8-0.35-SP3	Yield stress (Pa)	Dynamic	59.34	15.05	2.40
		Static	94.4	23.6	5.7
	Final viscosity (Pa.s)		3.71	1.40	0.61

It can be seen from Tables 10 and 11 that the rheological parameters of the C6 mixture have a higher value compared to the C5 mixture. It is understood from Table 2 that the C_3A contents of C5 and C6 cements are very close to each other, but the fineness value of C6 cement is 35% higher. The fineness of the C7 mixture is very close to that of the C5 mixture, but it contains two times more C_3A (Table 2). It is understood from Tables 10 and 12 that C5 mix is more successful than C7 mix in terms of rheological properties. It can be seen from Table 2, compared to C5 cement the Blaine specific surface and C_3A content are 24% and four times higher for C8 cement, respectively. It can be seen from Table 13 that C8 paste is the mixture with the lowest performance in terms of rheological properties after C4 mix.

Owing to the thixotropic character of paste, SYS of the mixtures was higher than their DYS. The difference between these two stress values was considerably high in the control mixtures. However, addition of the admixture resulted in reduction of the stresses and, meanwhile, reduced the difference between them. The fact was more pronounced in the pastes containing 0.2% admixture.

An exponential weak relationship between the SYS, obtained from the first period, and DYS obtained from the fourth period of deformation rate history is shown in Fig. 2. The main reason for such a weakness is the great difference between SYS and DYS values in the mixtures containing no or low admixture.

4.2 Evaluation of modeling results

4.2.1 Multiple additive regression trees and multiple adaptive regression splines modeling results

It is required to choose the variables such as the subsample fraction (SF), the number of trees to be constructed (NOT), the number of maximum nodes per tree (NOMN), maximum depth of tree (MDT), minimum terminal node (MTN) effectively in the analysis conducted with MART model. Different value estimations for these variables directly affect the accuracy of the model. Optimal parameters for the MART model used in this study were

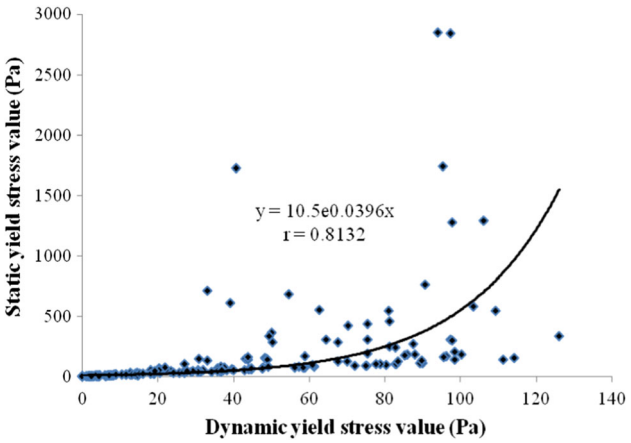


Fig. 2 Relationship between dynamic-static yield stresses of pastes

Table 14 Performance of MART models predicted DYS for different values of variables

Model	SF	NOT	NOMN	MDT	MTN	Training			Testing		
						RMSE	MAE	NSE	RMSE	MAE	NSE
1	0.5	1000	2	100,000	5	0.112	0.076	0.744	0.114	0.091	0.748
2	1.0	4000	2	100,000	5	0.112	0.075	0.743	0.111	0.088	0.760
3	0.5	7000	2	100,000	5	0.106	0.073	0.770	0.107	0.086	0.776
4	1.0	10,000	2	100,000	5	0.109	0.074	0.757	0.109	0.087	0.768
5	1.0	1000	5	50,000	10	0.089	0.054	0.836	0.085	0.064	0.859
6	0.5	4000	5	50,000	10	0.106	0.072	0.771	0.095	0.076	0.824
7	1.0	7000	5	50,000	10	0.079	0.045	0.873	0.078	0.060	0.881
8	0.5	10,000	5	50,000	10	0.094	0.059	0.817	0.093	0.072	0.832
9	0.5	1000	10	10,000	2	0.070	0.039	0.899	0.079	0.056	0.877
10	1.0	4000	10	10,000	2	0.056	0.028	0.937	0.088	0.068	0.849
11	0.5	7000	10	10,000	2	0.070	0.039	0.899	0.079	0.056	0.877
12	1.0	10,000	10	10,000	2	0.056	0.028	0.937	0.088	0.068	0.849
The best	**1.0**	**10,000**	**10**	**100,000**	**10**	**0.070**	**0.038**	**0.898**	**0.074**	**0.059**	**0.892**

Table 15 Performance of MART models predicted FV for different values of variables

Model	SF	NOT	NOMN	MDT	MTN	Training			Testing		
						RMSE	MAE	NSE	RMSE	MAE	NSE
1	0.5	1000	2	100,000	5	0.076	0.051	0.792	0.085	0.058	0.766
2	1.0	4000	2	100,000	5	0.076	0.050	0.791	0.085	0.057	0.769
3	0.5	7000	2	100,000	5	0.071	0.049	0.818	0.082	0.060	0.784
4	1.0	10,000	2	100,000	5	0.076	0.050	0.794	0.084	0.058	0.771
5	1.0	1000	5	50,000	10	0.061	0.033	0.867	0.072	0.046	0.833
6	0.5	4000	5	50,000	10	0.075	0.046	0.800	0.075	0.051	0.819
7	1.0	7000	5	50,000	10	0.050	0.026	0.911	0.064	0.044	0.866
8	0.5	10,000	5	50,000	10	0.068	0.040	0.831	0.072	0.051	0.832
9	0.5	1000	10	10,000	2	0.048	0.025	0.917	0.062	0.041	0.876
10	1.0	4000	10	10,000	2	0.036	0.012	0.953	0.059	0.042	0.888
11	0.5	7000	10	10,000	2	0.032	0.013	0.963	0.055	0.040	0.903
12	1.0	10,000	10	10,000	2	0.035	0.011	0.957	0.057	0.041	0.894
The best	**1.0**	**10,000**	**6**	**100,000**	**3**	**0.036**	**0.015**	**0.953**	**0.049**	**0.037**	**0.921**

determined through trial-and-error method. SF, NOT, NOMN, MDT, and MTN were chosen in the range of 0.5–1.0, 1000–10,000, 2–10, 1000–100,000, and 2–10, respectively. The performance of MART models for some different values of the variables used is presented in Tables 14 and 15 for DYS and FV, respectively.

The fundamental functions of MARS model and the equations obtained from these functions are shown in Table 16. As can be seen from the table, the number of fundamental functions used to estimate DYS and FV is 9 and 13, respectively. In the DYS equation, there are only six (out of nine) independent variables, i.e., C_3A, C_3S and C_4AF variables are not involved in the equation. On the other hand, the equation obtained from MARS model for FV estimation includes all of the variables except for C_2S.

In the MARS model, a two-step process was repeated until the desired model was obtained. The first step created all possible basic functions. The model was developed with basic functions added until a very large model was found, that is, until the complexity of the model reached its maximum level. By trimming the maximum model created in the second step, that is, by determining the important independent variables and the interactions of these variables, the most appropriate model with the sum of the squares of errors was formed [80]. As it can be seen from Table 16, the MARS model made an estimate without considering the C_3A value. However, according to the literature survey, the cement C_3A content is one of the major factors influencing fresh properties of the cementitious systems. In this context, the MARS model has also taken into account the C_3A parameter when creating the basic

Table 16 Basic functions and equations obtained from MARS for DYS and FV

DYS		FV	
BF3	max (0, AC−0.1)	BF1	max (0, AC−0.1)
BF4	max (0, W/C−0.1)	BF2	max (0, CF−0.701379)
BF6	max (0, 0.335988−C_2S)	BF3	max (0, 0.701379−CF)
BF7	max (0, ASC−0.800415) * BF3	BF4	max (0, W/C−0.1)
BF9	max (0, W/C−0.1) * BF3	BF5	max (0, C_3S−0.62)
BF11	max (0, 0.335988−C_2S) * BF9	BF7	max (0, CF−0.1) * BF4
BF12	max (0, CF−0.651724) * BF3	BF8	max (0, AC−0.1) * BF5
BF19	max (0, C_4AF−0.1) * BF7	BF9	max (0, AC−0.5) * BF4
BF20	max (0, ASC−0.1) * BF12	BF11	max (0, ASC−0.800415)
		BF12	max (0, 0.800415−ASC)
		BF13	max (0, C_3A−0.1) * BF12
		BF15	max (0, 0.654419−C4AF) * BF11
		BF16	max (0, EAC−0.1) * BF12

DYS = 0.751554–0.473695*BF3−0.221926*BF4−1.0682*BF6−1.7354*BF7 + 0.820356*BF11 + 2.51265*BF19 + 2.03677*BF20;

FV = 0.766557–0.547917*BF1 + 0.847303*BF2−0.28983*BF3−0.119142*BF4−0.926746*BF5
−0.26508*BF7 + 0.971937*BF8 + 0.276472*BF9−0.477424*BF13−2.4844*BF15 + 0.236388*BF16;

Table 17 Coefficients obtained from CRA for DYS

Models	Coefficients										
	w_0	w_1	w_2	w_3	w_4	w_5	w_6	w_7	w_8	w_9	w_{10}
LF	− 4.9028	0.6603	3.9152	2.7912	0.7804	2.5536	0.5973	− 0.4310	− 0.0179	− 0.2123	-
PF	0.7585	0.4419	0.4946	− 0.1145	0.0291	0.6074	0.0701	− 0.8921	0.5368	− 0.2197	-
EF	− 0.6738	− 3.4891	0.6252	2.7606	1.7506	0.3199	1.7945	0.4578	− 0.4475	0.0381	− 0.2191

$y_{LF} = w_0 + w_1X_1 + w_2X_2 + w_3X_3 + w_4X_4 + w_5X_5 + w_6X_6 + w_7X_7 + w_8X_8 + w_9X_9$

$y_{PF} = w_0X_1^{w_1}X_2^{w_2}X_3^{w_3}X_4^{w_4}X_5^{w_5}X_6^{w_6}X_7^{w_7}X_8^{w_8}X_9^{w_9}$

$y_{EF} = w_0 + \exp(w_1 + w_2X_1 + w_3X_2 + w_4X_3 + w_5X_4 + w_6X_5 + w_7X_6 + w_8X_7 + w_9X_8 + w_{10}X_9)$

Table 18 Coefficients obtained from CRA for FV

Models	Coefficients										
	w0	w1	w2	w3	w4	w5	w6	w7	w8	w9	w10
LF	− 2.3831	0.4593	2.3709	1.2234	0.0225	1.6001	0.3487	− 0.2865	− 0.0873	− 0.1733	-
PF	0.4954	0.4148	0.4845	− 0.3212	− 0.1623	0.7486	0.0604	− 0.7199	0.3559	− 0.2149	-
EF	− 0.0989	− 3.3892	1.0977	3.1892	0.4203	− 1.2233	2.2144	0.5350	− 0.8000	− 0.0198	− 0.4583

$y_{LF} = w_0 + w_1X_1 + w_2X_2 + w_3X_3 + w_4X_4 + w_5X_5 + w_6X_6 + w_7X_7 + w_8X_8 + w_9X_9$

$y_{PF} = w_0X_1^{w_1}X_2^{w_2}X_3^{w_3}X_4^{w_4}X_5^{w_5}X_6^{w_6}X_7^{w_7}X_8^{w_8}X_9^{w_9}$

$y_{EF} = w_0 + \exp(w_1 + w_2X_1 + w_3X_2 + w_4X_3 + w_5X_4 + w_6X_5 + w_7X_6 + w_8X_7 + w_9X_8 + w_{10}X_9)$

functions. However, the model found that C_3A had a low contribution in improving model accuracy compared to other parameters. Therefore, the MARS model neglected the C_3A effect, which also considers model complexity. As it can be seen from Table 24 in contrast to the MARS model, MART model took into account the C_3A content along with the other important parameters. The fact seems to be an indication of superiority of the MART model to MARS model in the estimation of paste rheological characteristics.

4.2.2 Conventional regression analysis and ANN results

In order to control the accuracy of the heuristic regression methods, conventional regression analysis (CRA) including linear, power, and exponential functions was also used to

Table 19 Performance values of ANN models predicted DYS for different neuron numbers of the hidden layer

Number of neuron	Training			Testing		
	RMSE	MAE	NS	RMSE	MAE	NS
2	0.0667	0.0501	0.9088	0.1096	0.0818	0.7656
3	**0.0530**	**0.0391**	**0.9423**	**0.0866**	**0.0631**	**0.8534**
4	0.0557	0.0364	0.9364	0.1086	0.0854	0.7696
5	0.0399	0.0254	0.9674	0.1167	0.0894	0.7343
6	0.0386	0.0243	0.9695	0.1420	0.1037	0.6060
7	0.0365	0.0187	0.9726	0.1588	0.1169	0.5076
8	0.0362	0.0182	0.9732	0.1714	0.1157	0.4262
9	0.0379	0.0196	0.9706	0.1667	0.1064	0.4571
10	0.0372	0.0183	0.9716	0.0372	0.1106	0.5104

Table 20 Performance values of ANN models predicted FV for different neuron numbers of the hidden layer

Number of neuron	Training			Testing		
	RMSE	MAE	NS	RMSE	MAE	NS
2	0.0383	0.0300	0.9470	0.0771	0.0567	0.8073
3	0.0325	0.0242	0.9620	0.0767	0.0537	0.8096
4	0.0280	0.0189	0.9718	0.0613	0.0452	0.8784
5	**0.0249**	**0.0160**	**0.9776**	**0.0572**	**0.0381**	**0.8941**
6	0.0192	0.0113	0.9867	0.1042	0.0729	0.6480
7	0.2280	0.0130	0.9812	0.0702	0.0499	0.8405
8	0.0229	0.0131	0.9810	0.1082	0.0693	0.6204
9	0.0227	0.0131	0.9814	0.0798	0.0577	0.7939
10	0.0224	0.0121	0.09818	0.1070	0.0768	0.6254

Table 21 RMSE, MAE and NS values of CRA, MARS, MART and ANN in training and testing set for DYS

Data set	Training						Testing					
Model	LF	PF	EF	MARS	MART	ANN	LF	PF	EF	MARS	MART	ANN
RMSE	0.103	0.105	0.100	0.096	0.070	**0.053**	0.104	0.108	0.101	0.086	**0.074**	0.087
MAE	0.080	0.081	0.078	0.077	**0.038**	0.039	0.084	0.086	0.083	0.067	**0.059**	0.063
NS	0.784	0.776	0.794	0.809	0.898	**0.942**	0.788	0.772	0.799	0.857	**0.892**	0.853

Table 22 RMSE, MAE and NS values of CRA, MARS, MART and ANN in training and testing set for FV

Data set	Training						Testing					
Model	LF	PF	EF	MARS	MART	ANN	LF	PF	EF	MARS	MART	ANN
RMSE	0.066	0.057	0.056	0.045	0.036	**0.025**	0.077	0.066	0.061	0.057	**0.049**	0.057
MAE	0.054	0.043	0.044	0.034	**0.015**	0.016	0.064	0.051	0.045	0.046	**0.037**	0.038
NS	0.844	0.885	0.886	0.928	0.953	**0.978**	0.806	0.858	0.880	0.894	**0.921**	0.894

estimate DYS and FV values. The optimal coefficients obtained by CRA regression functions are shown in Tables 17 and 18 for DYS and FV, respectively.

In the ANN model, the optimum number of neurons for the hidden layer was found by trial and error. The number of hidden neurons was chosen between 2 and 10 in increments of one. The maximum iteration number was adjusted to 10,000. For activation of the hidden and output layers of the network, hyperbolic tangent sigmoid transfer function (tansig) and linear transfer function (purelin) were used,

respectively. In the ANN models, the learning coefficient 0.8 and the momentum coefficient 1.0 were considered. Performance values of ANN models for different neuron numbers of the hidden layer are given in Tables 19 and 20 for DYS and FV, respectively. In the tables, the best ANN model is presented in bold.

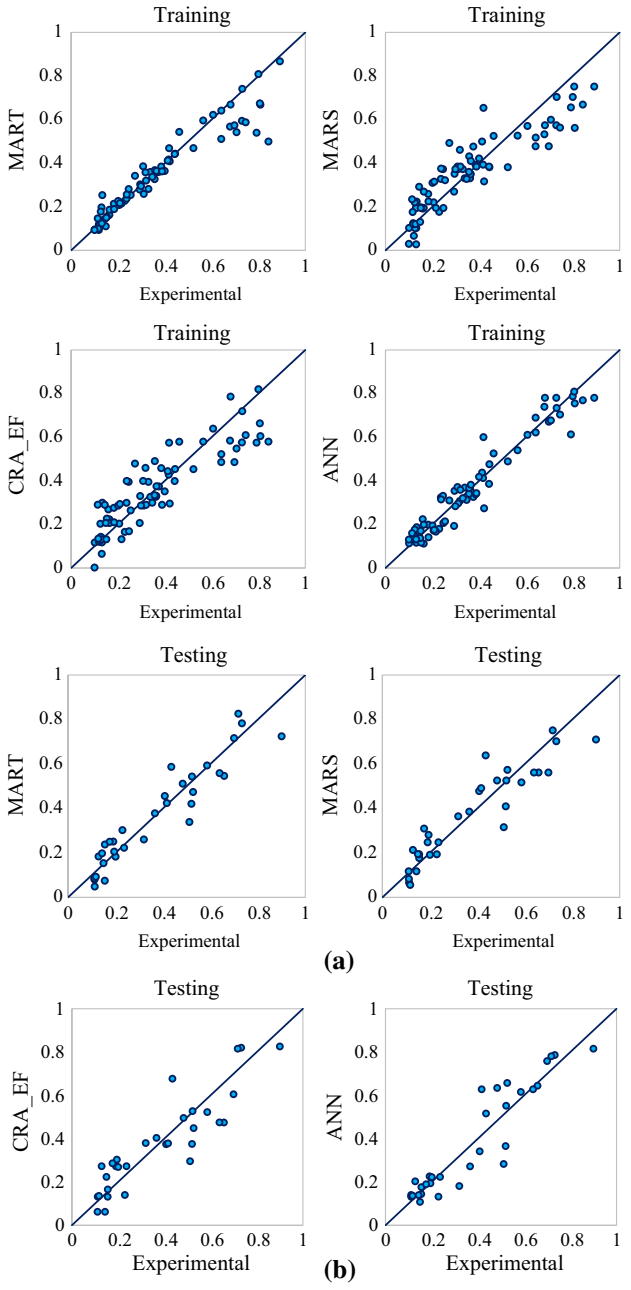


Fig. 3 Scatter plots of the experimental results with the estimated ones by the MART, MARS, and CRA-EF for **a** training and **b** testing data sets for DYS

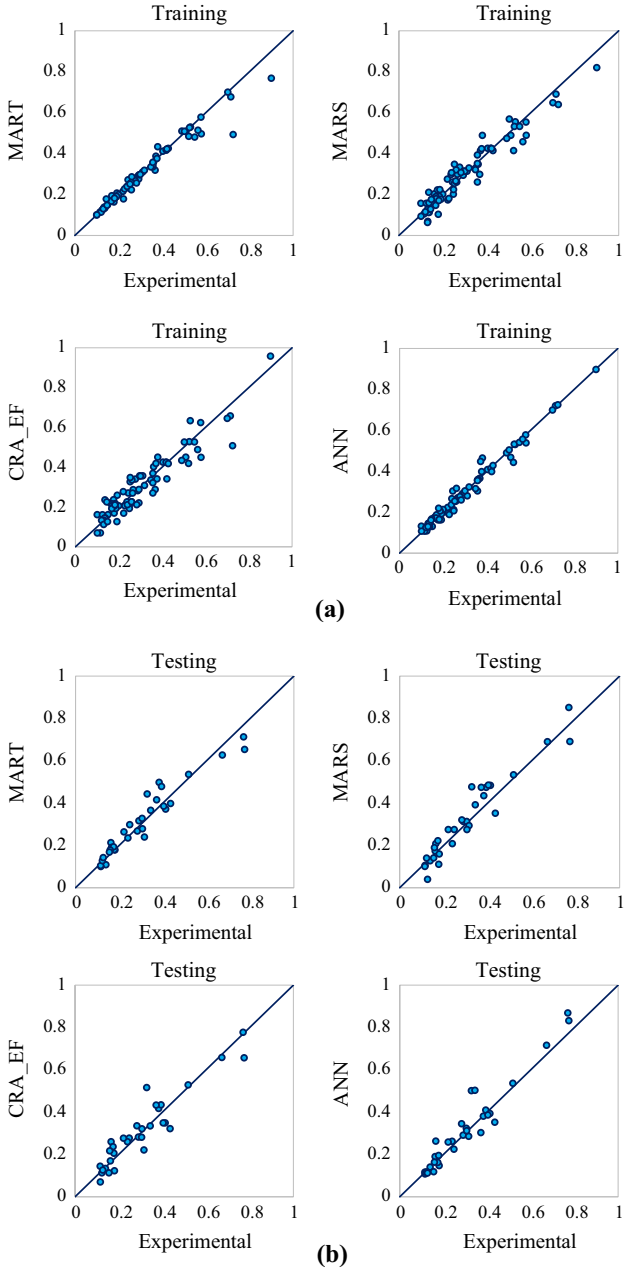


Fig. 4 Scatter plots of the experimental results with the estimated ones by the MART, MARS, and CRA-EF for **a** training and **b** testing data sets for FV

4.2.3 Comparing MART and MARS modeling results with results of CRA and ANN

The results of CRA and ANN models were used to evaluate the DYS and FV estimation abilities of MART and MARS models. RMSE, MAE, and NS values for each of the three models are presented in Tables 21 and 22 for DYS and FV values, respectively. Models were compared using the errors and NS values presented in these tables. The results

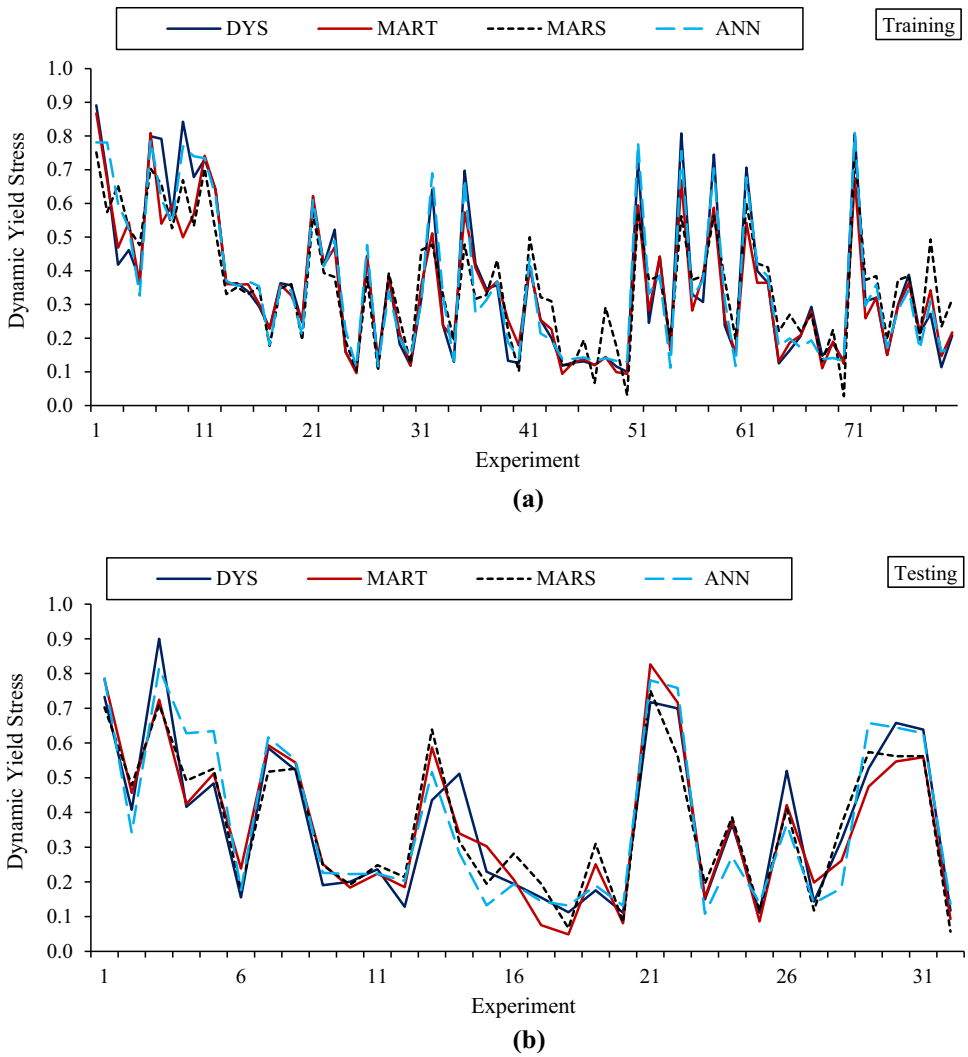


Fig. 5 Comparison of the experimental DYS values with the predicted ones by the MART and MARS for **a** training and **b** test sets

displaying the lowest error values for DYS and FV (the highest NS value) were marked in bold.

The lowest MAE values for both of the variables were obtained from the MART model in both the training and testing set. While the performance of the MART model was better in the testing set in terms of RMSE and NS values, the performance of the ANN model was better in the training set. RMSE, MAE, and NS values for the testing set in MART model designed for DYS estimation were determined as 0.074, 0.059, and 0.892, respectively. When the RMSE value is examined, the MART model appeared to be about 14% better than the MARS and ANN models and about 27% better than the CRA-EF for the testing set. In MART model designed for FV estimation, RMSE, MAE, and NS values in the testing set were determined as 0.049, 0.037, and 0.921, respectively. It can be observed from NS values that estimation of FV values is more accurate than that of DYS values. The MART model is 14 to 36% superior to the other models when RMSE values for the testing set are taken into account.

According to the NS values, if the models are evaluated in both training and testing sets for DYS and FV, the models can be classified as very good because the NS value is above 0.75 in all models. The closer the NS value is to 1, the higher the model performance will be. Therefore, higher NS values in FV prediction models than DYS models reveal that DYS values are modeled with greater accuracy.

Even though the MARS and ANN models results were somewhat worse than those of the MART model for testing set, these models performed better than any CRA model. Although the ANN and MARS models for the test set gave close results, the ANN model for the training set showed better results than the other models. Among the CRA models, exponential function showed the best performance either in the training or in the testing set. The exponential

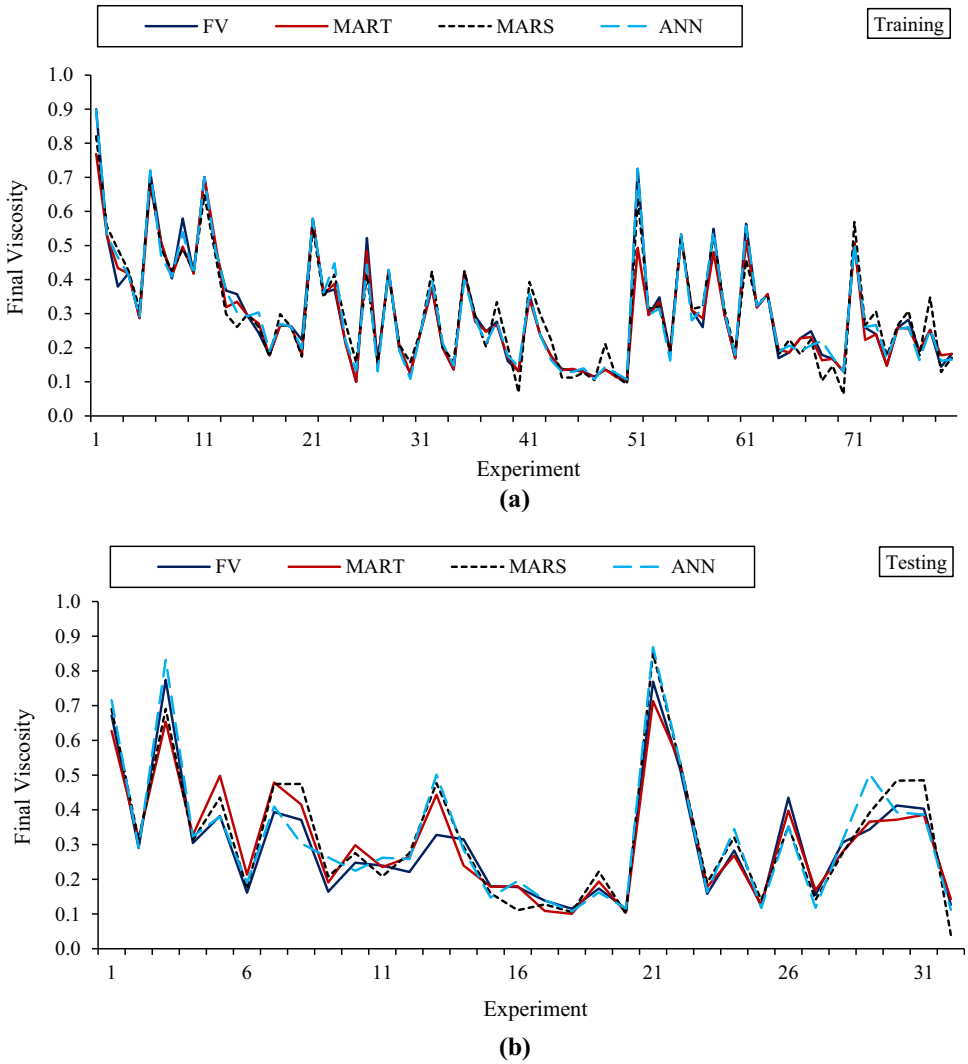


Fig. 6 Comparison of the experimental FV values with the predicted ones by the MART and MARS for **a** training and **b** test sets

Table 23 Validity limits of the models

Limit	CF (cm^2/g)	C_3A (%)	C_3S (%)	C_2S (%)	C_4AF (%)	EAC (%)	AC (%)	ASC (%)	W/C
Minimum	2810	1.90	52.50	10.20	7.67	0.50978	0	0	0.32
Maximum	4260	13.88	67.10	20.37	16.27	1.23220	0.2	38.56	0.35

function was followed by the power and linear functions, respectively.

Scatter diagrams of the EF-CRA (the best model of CRA), MART, MARS, and ANN models are shown in Figs. 3 and 4 for DYS and FV values, respectively. It can be seen from Fig. 3 that, owing to its best performance, the scattering of the MART model was the lowest in the test set, while the ANN model gave the smallest scatter in the training set.

From Fig. 4, it is obvious that in both of the training and testing sets the scatter of the FV values is lower than that of the DYS values. The greater NS values of FV than those of DYS support the feature. Moreover, Fig. 4 reveals that the closest values to 45° line in the training and testing sets are obtained from the ANN and MART models, respectively.

The experimental values of DYS and FV are compared with the corresponding values obtained from the MARS, MART, and ANN models by the time series diagrams shown in Figs. 5 and 6, respectively.

Although the models gave very good results, the coefficients of the models were obtained using limited experimental data. Therefore, it should be noted that the validity limits of the models are as given in Table 23.

Table 24 Relative importance of the input variables on (a) DYS and (b) FV in the MART

(a) Variable importance for DYS (%)		
AC	100	
CF	98.18	
ASC	78.99	
C3S	77.71	
W/C	69.77	
C3A	59.48	
EAC	45.75	
C4AF	43.65	
C2S	28.51	
(b) Variable importance for FV (%)		
ASC	100	
AC	99.78	
CF	96.77	
W/C	87.26	
C3A	76.24	
C3S	74.69	
C4AF	47.97	
EAC	39.78	
C2S	28.08	

4.2.4 Relative importance of the input variables

One of the advantages provided by the MART model, which showed the best performance among the models used in the present study, is the possibility to determine the relative importance of any input variable by assigning a value in between 0 and 100. Although the MARS model displays a similar analysis, the relative importance values obtained from the MART model are merely presented in Table 24.

According to the results given in Table 24, all of the input variables were found to be effective on the rheological properties of the paste, but in different relative importance varying between 28 and 100%. Compared to the other parameters, AC and CF with the highest relative importance values (100% and 98%, respectively) were the most effective ones on the DYS. These were followed by ASC and C_3S content with their relative importance values exceeding 75%. C_2S was determined as the least effective parameter on the DYS with its 28% relative importance. On the other hand, ASC, AC, and CF (having relative importance in the range of 97 to 100%) were the most important parameters affecting the FV of pastes. In this regard, W/C, C_3A, and C_3S contents were determined as the other effective parameters with their relative importance levels over 70%. Once again, C_2S content was confirmed as the least affecting parameter on the FV with its 28% relative importance.

Interestingly, the admixture content, cement fineness, and admixture solid material content were determined to have greater influence on the paste rheological properties than that of the mineralogical composition of cement. Fineness of cement was found to be the most effective cement characteristic on the paste rheology.

5 Conclusion

The compatibility between CEMI portland cements and polycarboxylate ether-based superplasticizers was investigated. It was focused particularly on the cement-based factors affecting the rheological properties of the paste mixtures. The dynamic yield stress and final viscosity of the pastes were determined experimentally and modeled using conventional and heuristic regression methods and artificial neural network. The following conclusions were drawn:

The most effective parameters on the dynamic yield stress of the pastes were (in decreasing order) admixture content of the mix, cement fineness, admixture solid content, C_3S content, water/cement ratio, C_3A, and equivalent alkali content of the cement. However, the admixture solid material content, admixture content of the mix, cement fineness, water/cement ratio as well as C_3A and C_3S contents of cement were the major influential factors on the paste final viscosity. Among the cement characteristics, fineness was determined to be the most effective property on the rheological properties of the pastes.

According to the modeling results, the multiple additive regression trees (MART) method presented the best estimations in testing sets than those of multivariate adaptive regression splines (MARS), conventional regression analysis (CRA) and artificial neural network (ANN) models. Considering the RMSE and NS values, the ANN model gave better results than the other models in the training set. According to RMSE values in the testing set, MART model provided 14 to 27% better estimation of the dynamic yield stress as well as 14 to 36% better estimation of final viscosity than those of other models. In the classification made according to NS values, all models for both FV and DYS were in very good class. However, according to the test set data, which is the data that the models did not see while training, the NS values were the highest in the MART model in both parameter estimates. For this reason, it is recommended to use MART model in FV and DYS estimation. The MART model seems to be appropriate for modeling of the rheological properties of the cementitious systems in future studies.

Acknowledgement The authors would like to express sincere thanks to Oyak, BatiÇim, Çimentaş, Akçansa, and Nuh cement plants as well as Draco, BASF, and Inka admixture companies for providing the cements and admixtures used in this study. The first author would also acknowledge the financial support provided by Turkish Cement Manufacturers Association during his PhD study.

Compliance with ethical standards

Conflict of interest None of the authors has any conflicts of interest to declare.

References

1. Tagnit-Hamou A, Aïtcin PC (1993) Cement and superplasticizer compatibility. World Cem 38–42
2. Schatzmann M, Fischer P, Bezzola GR (2003) Rheological behavior of fine and large particle suspensions. J Hydraul Eng 129:796–803. https://doi.org/10.1061/(ASCE)0733-9429(2003)129:10(796)
3. Schatzmann M, Bezzola GR, Fischer P, et al (2004) The ball measuring system-a new rheometric tool to determine the flow curve of large particle material. In: Swiss Group of Rheology Annual Meeting. Lausanne/Switzerland
4. Koehler E, Fowler D (2004) Development of a Portable rheometer for fresh Portland cement concrete. Int Cent Aggregates Res 321
5. Özen S, Altun MG, Mardani-Aghabaglou A (2020) Effect of the polycarboxylate based water reducing admixture structure on self-compacting concrete properties: main chain length. Constr Build Mater 255:119360. https://doi.org/10.1016/j.conbuildmat.2020.119360
6. Altun MG, Özen S, Mardani-Aghabaglou A (2020) Effect of side chain length change of polycarboxylate-ether based high range water reducing admixture on properties of self-compacting concrete. Constr Build Mater 246:118427. https://doi.org/10.1016/j.conbuildmat.2020.118427
7. Hanehara S, Yamada K (1999) Interaction between cement and chemical admixture from the point of cement hydration, absorption behaviour of admixture, and paste rheology. Cem Concr Res 29:1159–1165. https://doi.org/10.1016/S0008-8846(99)00004-6
8. Dodson VH, Hayden TD (1989) Another look at the Portland cement/chemical admixture incompatibility problem. Cem Concr Aggregates 11:52–56
9. Bonen D, Sarkar SL (1995) The superplasticizer adsorption capacity of cement pastes, pore solution composition, and parameters affecting flow loss. Cem Concr Res 25:1423–1434. https://doi.org/10.1016/0008-8846(95)00137-2
10. Jiang S, Kim BG, Aïtcin PC (1999) Importance of adequate soluble alkali content to ensure cement/superplasticizer compatibility. Cem Concr Res 29:71–78. https://doi.org/10.1016/S0008-8846(98)00179-3
11. Erdogdu S (2000) Compatibility of superplasticizers with cements different in composition. Cem Concr Res 30:767–773. https://doi.org/10.1016/S0008-8846(00)00229-5
12. Bedard C, Mailvaganam NP (2005) The use of chemical admixtures in concrete. Part II: Admixture-admixture compatibility and practical problems. J Perform Constr Facil 19:263–266. https://doi.org/10.1061/(ASCE)0887-3828(2005)19:4(263)
13. Ramachandran VS (1995) Concrete admixtures handbook. Noyes Publications, New Jersey
14. Ramachandran VS (2002) Concrete admixtures handbook. Standard Publishers, New Delhi
15. Uchikawa H, Hanehara S, Shirasaka T, Sawaki D (1992) Effect of admixture of hydration of cement, adsorptive behaviour of admixture and fluidity and setting of fresh cement paste. Cem Concr Res 22:1115–1129
16. Yousuf M, Mollah A, Palta P et al (1995) Chemical and physical effects of sodium lignosulfonate superplasticizer on the hydration of portland cement and solidification/stabilization consequences. Cem Concr Res. https://doi.org/10.1016/0008-8846(95)00055-H
17. Rixom R, Mailvaganam N (1999) Chemical admixtures for concrete. E&FN Spon, London
18. Flatt RJ, Houst YF (2001) A simplified view on chemical effects perturbing the action of superplasticizers. Cem Concr Res 31:1169–1176. https://doi.org/10.1016/S0008-8846(01)00534-8
19. Griesser A (2002) Cement-superplasticizer ınteractions at ambient temperatures; rheology, phase composition, pore water and heat of hydration of cementitious systems. Swiss Federal Institute of Technology
20. Mardani-Aghabaglou A, Tuyan M, Yilmaz G et al (2013) Effect of different types of superplasticizer on fresh, rheological and strength properties of self-consolidating concrete. Constr Build Mater 47:1020–1025. https://doi.org/10.1016/j.conbuildmat.2013.05.105
21. Aïtcin PC (2004) High performance concrete. E&FN SPON, New York
22. Prince W, Edwards-Lajnef M, Aïtcin PC (2002) Interaction between ettringite and a polynaphthalene sulfonate superplasticizer in a cementitious paste. Cem Concr Res 32:79–85. https://doi.org/10.1016/S0008-8846(01)00632-9
23. Vernet C, Noworyta G (1992) Reactivity test for fine silicas and pozzolonic mineral additives. In: Proceedings of the 9th ınternational congress on the chemistry of cement Vol. III. New Delhi, pp 79–85
24. Burgos-Montes O, Palacios M, Rivilla P, Puertas F (2012) Compatibility between superplasticizer admixtures and cements with mineral additions. Constr Build Mater 31:300–309. https://doi.org/10.1016/j.conbuildmat.2011.12.092
25. Gołaszewski J (2012) Influence of cement properties on new generation superplasticizers performance. Constr Build Mater 35:586–596. https://doi.org/10.1016/j.conbuildmat.2012.04.070
26. He T, Shi C, Li G, Song X (2012) Effects of superplasticizers on the carbonation resistance of C 3S and C 3A hydration products. Constr Build Mater 36:954–959. https://doi.org/10.1016/j.conbuildmat.2012.06.071
27. Sonebi M, Lachemi M, Hossain KMA (2013) Optimisation of rheological parameters and mechanical properties of superplasticised cement grouts containing metakaolin and viscosity modifying admixture. Constr Build Mater 38:126–138. https://doi.org/10.1016/j.conbuildmat.2012.07.102
28. Ouyang X, Jiang X, Qiu X et al (2009) Effect of molecular weight of sulfanilic acid-phenol-formaldehyde condensate on the properties of cementitious system. Cem Concr Res 39:283–288. https://doi.org/10.1016/j.cemconres.2009.01.002
29. Alonso MM, Palacios M, Puertas F (2013) Compatibility between polycarboxylate-based admixtures and blended-cement pastes. Cem Concr Compos 35:151–162. https://doi.org/10.1016/j.cemconcomp.2012.08.020
30. Özcan F, Atiş CD, Karahan O et al (2009) Comparison of artificial neural network and fuzzy logic models for prediction of long-term compressive strength of silica fume concrete. Adv Eng Softw 40:856–863. https://doi.org/10.1016/j.advengsoft.2009.01.005
31. Saridemir M, Topçu IB, Özcan F, Severcan MH (2009) Prediction of long-term effects of GGBFS on compressive strength of concrete by artificial neural networks and fuzzy logic. Constr

Build Mater 23:1279–1286. https://doi.org/10.1016/j.conbuildmat.2008.07.021
32. Zhang J, Ma G, Huang Y et al (2019) Modelling uniaxial compressive strength of lightweight self-compacting concrete using random forest regression. Constr Build Mater 210:713–719. https://doi.org/10.1016/j.conbuildmat.2019.03.189
33. Amlashi AT, Abdollahi SM, Goodarzi S, Ghanizadeh AR (2019) Soft computing based formulations for slump, compressive strength, and elastic modulus of bentonite plastic concrete. J Clean Prod 230:1197–1216. https://doi.org/10.1016/j.jclepro.2019.05.168
34. Asteris PG, Mokos VG (2020) Concrete compressive strength using artificial neural networks. Neural Comput Appl 32:11807–11826. https://doi.org/10.1007/s00521-019-04663-2
35. Saha P, Debnath P, Thomas P (2020) Prediction of fresh and hardened properties of self-compacting concrete using support vector regression approach. Neural Comput Appl 32:7995–8010. https://doi.org/10.1007/s00521-019-04267-w
36. Selvaraj S, Sivaraman S (2019) Prediction model for optimized self-compacting concrete with fly ash using response surface method based on fuzzy classification. Neural Comput Appl 31:1365–1373. https://doi.org/10.1007/s00521-018-3575-1
37. Ashrafian A, Shokri F, Taheri Amiri MJ et al (2020) Compressive strength of foamed cellular lightweight concrete simulation: new development of hybrid artificial intelligence model. Constr Build Mater 230:117048. https://doi.org/10.1016/j.conbuildmat.2019.117048
38. Chou JS, Chiu CK, Farfoura M, Al-Taharwa I (2011) Optimizing the prediction accuracy of concrete compressive strength based on a comparison of data-mining techniques. J Comput Civ Eng 25:242–253
39. Yuan Z, Wang LN, Ji X (2014) Prediction of concrete compressive strength: Research on hybrid models genetic based algorithms and ANFIS. Adv Eng Softw 67:156–163. https://doi.org/10.1016/j.advengsoft.2013.09.004
40. Dutta S, Ramachandra Murthy A, Kim D, Samui P (2017) Prediction of compressive strength of self-compacting concrete using intelligent computational modeling. Comput Mater Contin 53:167–185
41. Eskandari-Naddaf H, Kazemi R (2017) ANN prediction of cement mortar compressive strength, influence of cement strength class. Constr Build Mater 138:1–11. https://doi.org/10.1016/j.conbuildmat.2017.01.132
42. Yaseen ZM, Deo RC, Hilal A et al (2018) Predicting compressive strength of lightweight foamed concrete using extreme learning machine model. Adv Eng Softw 115:112–125. https://doi.org/10.1016/j.advengsoft.2017.09.004
43. Al-Shamiri AK, Kim JH, Yuan TF, Yoon YS (2019) Modeling the compressive strength of high-strength concrete: an extreme learning approach. Constr Build Mater 208:204–219. https://doi.org/10.1016/j.conbuildmat.2019.02.165
44. Ghanizadeh AR, Abbaslou H, Amlashi AT, Alidoust P (2019) Modeling of bentonite/sepiolite plastic concrete compressive strength using artificial neural network and support vector machine. Front Struct Civ Eng 13:215–239. https://doi.org/10.1007/s11709-018-0489-z
45. Nguyen T, Kashani A, Ngo T, Bordas S (2019) Deep neural network with high-order neuron for the prediction of foamed concrete strength. Comput Civ Infrastruct Eng 34:316–332. https://doi.org/10.1111/mice.12422
46. Hoang ND, Tran XL, Nguyen H (2020) Predicting ultimate bond strength of corroded reinforcement and surrounding concrete using a metaheuristic optimized least squares support vector regression model. Neural Comput Appl 32:7289–7309. https://doi.org/10.1007/s00521-019-04258-x
47. Xu J, Zhao X, Yu Y et al (2019) Parametric sensitivity analysis and modelling of mechanical properties of normal- and high-strength recycled aggregate concrete using grey theory, multiple nonlinear regression and artificial neural networks. Constr Build Mater 211:479–491. https://doi.org/10.1016/j.conbuildmat.2019.03.234
48. Gholampour A, Mansouri I, Kisi O, Ozbakkaloglu T (2020) Evaluation of mechanical properties of concretes containing coarse recycled concrete aggregates using multivariate adaptive regression splines (MARS), M5 model tree (M5Tree), and least squares support vector regression (LSSVR) models. Neural Comput Appl 32:295–308. https://doi.org/10.1007/s00521-018-3630-y
49. Cheng MY, Cao MT (2016) Estimating strength of rubberized concrete using evolutionary multivariate adaptive regression splines. J Civ Eng Manag 22:711–720. https://doi.org/10.3846/13923730.2014.897989
50. Karthiyaini S, Senthamaraikannan K, Priyadarshini J et al (2019) Prediction of mechanical strength of fiber admixed concrete using multiple regression analysis and artificial neural network. Adv Mater Sci Eng. https://doi.org/10.1155/2019/4654070
51. Ashrafian A, Taheri Amiri MJ, Rezaie-Balf M et al (2018) Prediction of compressive strength and ultrasonic pulse velocity of fiber reinforced concrete incorporating nano silica using heuristic regression methods. Constr Build Mater 190:479–494. https://doi.org/10.1016/j.conbuildmat.2018.09.047
52. Kaveh A, Bakhshpoori T, Hamze-Ziabari SM (2018) M5' and mars based prediction models for properties of selfcompacting concrete containing fly ash. Period Polytech Civ Eng 62:281–294. https://doi.org/10.3311/PPci.10799
53. Rezaie M, Sadighi N (2017) Prediction of slump and density of lightweight concretes using ANFIS and linear regression. Int J Civ Eng Technol 8:1635–1648
54. Yu Y, Zhang C, Gu X, Cui Y (2019) Expansion prediction of alkali aggregate reactivity-affected concrete structures using a hybrid soft computing method. Neural Comput Appl 31:8641–8660. https://doi.org/10.1007/s00521-018-3679-7
55. Sezer A, Sezer Gİ, Mardani-Aghabaglou A, Altun S (2020) Prediction of mechanical and penetrability properties of cement-stabilized clay exposed to sulfate attack by use of soft computing methods. Neural Comput Appl. https://doi.org/10.1007/s00521-020-04972-x
56. Sadowski Ł, Nikoo M, Shariq M et al (2019) The nature-ınspired metaheuristic method for predicting the creep strain of green concrete containing ground granulated blast furnace slag. Mater (Basel). https://doi.org/10.3390/ma12020293
57. Shahriar A, Nehdi ML (2013) Modelling rheological properties of oil well cement slurries using multiple regression analysis and artificial neural networks. J Mater Civ Eng 3:26–37
58. Friedman JH (1991) Multivariate adaptive regression splines (with Discussion). Ann Stat 19:1–141. https://doi.org/10.1214/aos/1176347969
59. Zhang W, Goh ATC (2016) Multivariate adaptive regression splines and neural network models for prediction of pile drivability. Geosci Front. https://doi.org/10.1016/j.gsf.2014.10.003
60. Tiryaki S, Tan H, Bardak S et al (2019) Performance evaluation of multiple adaptive regression splines, teaching–learning based optimization and conventional regression techniques in predicting mechanical properties of impregnated wood. Eur J Wood Wood Prod 77:645–659. https://doi.org/10.1007/s00107-019-01416-9
61. Friedman JH, Meulman JJ (2003) Multiple additive regression trees with application in epidemiology. Stat Med 22:1365–1381. https://doi.org/10.1002/sim.1501
62. Fu J-C, Huang H-Y, Jang J-H, Huang P-H (2019) River stage forecasting using multiple additive regression trees. Water

Resour Manag 33:4491–4507. https://doi.org/10.1007/s11269-019-02357-x
63. Felekoğlu B (2014) Rheological behaviour of self-compacting micro-concrete. Sadhana Acad Proc Eng Sci 39:1471–1495. https://doi.org/10.1007/s12046-014-0281-2
64. Mardani-Aghabaglou A, Boyaci OC, Hosseinnezhad H et al (2016) Effect of gypsum type on properties of cementitious materials containing high range water reducing admixture. Cem Concr Compos 68:15–26. https://doi.org/10.1016/j.cemconcomp.2016.02.007
65. Mardani-Aghabaglou A, Felekoğlu B, Ramyar K (2017) Effect of cement C3A content on properties of cementitious systems containing high-range water-reducing admixture. J Mater Civ Eng 29:1–12. https://doi.org/10.1061/(ASCE)MT.1943-5533.0001925
66. Mardani-Aghabaglou A, Son AE, Felekoglu B, Ramyar K (2017) Effect of cement fineness on properties of cementitious materials containing high range water reducing admixture. J Green Build 12:142–167. https://doi.org/10.3992/1552-6100.12.1.142
67. Bayram A, Uzlu E, Kankal M, Dede T (2015) Modeling stream dissolved oxygen concentration using teaching–learning based optimization algorithm. Environ Earth Sci 73:6565–6576. https://doi.org/10.1007/s12665-014-3876-3
68. Kankal M, Yüksek Ö (2014) Artificial neural network for estimation of harbor oscillation in a cargo harbor basin. Neural Comput Appl. https://doi.org/10.1007/s00521-013-1451-6
69. Bayram A, Kankal M (2015) Artificial neural network modeling of dissolved oxygen concentration in a Turkish watershed. Polish J Environ Stud 24:1507–1515
70. Nacar S, Hınıs MA, Kankal M (2018) Forecasting daily streamflow discharges using various neural network models and training algorithms. KSCE J Civ Eng. https://doi.org/10.1007/s12205-017-1933-7
71. Uzlu E, Akpinar A, Özturk HT et al (2014) Estimates of hydroelectric generation using neural networks with the artificial bee colony algorithm for Turkey. Energy. https://doi.org/10.1016/j.energy.2014.03.059
72. Suman S (2015) Prediction of pile capacity parameters using functional networks and multivariate adaptive regression splines. National Institute of Technology
73. Samui P (2013) Multivariate adaptive regression spline (MARS) for prediction of elastic modulus of jointed rock mass. Geotech Geol Eng 31:249–253. https://doi.org/10.1007/s10706-012-9584-4
74. Khuntia S, Mujtaba H, Patra C et al (2015) Prediction of compaction parameters of coarse grained soil using multivariate adaptive regression splines (MARS). Int J Geotech Eng 9:79–88. https://doi.org/10.1179/1939787914Y.0000000061
75. Dey P, Das AK (2016) Application of multivariate adaptive regression spline-assisted objective function on optimization of heat transfer rate around a cylinder. Nucl Eng Technol 48:1315–1320. https://doi.org/10.1016/J.NET.2016.06.011
76. Friedman JH (2001) Estimation of daily streamflow using multivariate adaptive regression splines. Ann Stat 29:1189–1232
77. Chen L, Peng S, Yang B (2015) Predicting alien herb invasion with machine learning models: biogeographical and life-history traits both matter. Biol Invasions 17:2187–2198. https://doi.org/10.1007/s10530-015-0870-y
78. Li B, Goel PK (2007) Additive regression trees and smoothing splines—predictive modeling and interpretation in data mining
79. Moriasi DN, Arnold JG, Van Liew MW et al (2007) Model evaluation guidelines for systematic quantification of accuracy in watershed simulations. Trans ASABE 50:885–900. https://doi.org/10.13031/2013.23153
80. Nacar S, Kankal M, Hınıs MA (2018) Estimation of daily streamflow using multivariate adaptive regression splines (MARS): a case study of Haldizen Stream. Gümüşhane Univ J Sci Technol Inst 8:38–47. https://doi.org/10.17714/gumusfenbil.311188

Publisher's Note Springer Nature remains neutral with regard to jurisdictional claims in published maps and institutional affiliations.